2. Lecture – Contents

- Strong (resonant) scattering, (generalized) T-Matrix

  wave functions, scattering phase shifts

2. Lecture – Contents

- Strong (resonant) scattering, (generalized) T-Matrix

  wave functions, scattering phase shifts
- δ-function scatterers and finite band width; graphene
- Comments on real space calculations on a lattice

T-Matrix

Schrödinger equation in integral form:

$$\psi_{\boldsymbol{k}}(\boldsymbol{r}) = \varphi_{\boldsymbol{k}}(\boldsymbol{r}) + \int d^D\rho\, G^0(\boldsymbol{r}-\boldsymbol{\rho}, \varepsilon(\boldsymbol{k}))\, V(\boldsymbol{\rho})\, \psi_{\boldsymbol{k}}(\boldsymbol{\rho})$$

Defining the T-Matrix: $T(\boldsymbol{p},\boldsymbol{k}) = \int d^D\rho\, \varphi^*_{\boldsymbol{p}}(\boldsymbol{\rho})\, V(\boldsymbol{\rho})\; \psi_{\boldsymbol{k}}(\boldsymbol{\rho})$

leads to $\psi_{\boldsymbol{k}}(\boldsymbol{r}) = \varphi_{\boldsymbol{k}}(\boldsymbol{r}) + \int \frac{d^D p}{(2\pi)^D}\, \varphi_{\boldsymbol{p}}(\boldsymbol{r})\; \hat{G}^0(\boldsymbol{p}, \varepsilon(\boldsymbol{k}))\; T(\boldsymbol{p},\boldsymbol{k})$

from which

$$T(\boldsymbol{k},\boldsymbol{k'}) = V(\boldsymbol{k}-\boldsymbol{k'}) + \int \frac{d^D p}{(2\pi)^D} V(\boldsymbol{k}-\boldsymbol{p})\; G^0\left(\boldsymbol{p}, \varepsilon(\boldsymbol{k'})\right)\; T(\boldsymbol{p},\boldsymbol{k'})$$

follows!

From the wave function $\psi_{\boldsymbol{k}}(\boldsymbol{r})$ we can construct the Green Function

$$G_E(\boldsymbol{r},\boldsymbol{r'}) = \int \frac{d^D k}{(2\pi)^D} \frac{\psi_{\boldsymbol{k}}(\boldsymbol{r})\,\psi_{\boldsymbol{k}}(\boldsymbol{r'})}{E + i\delta - \varepsilon(\boldsymbol{k})}$$

$-\frac{1}{\pi}\,\mathcal{I}m\,G_E(\boldsymbol{r},\boldsymbol{r}) = \mathcal{N}(\boldsymbol{r},E)$ is the Local Density of States (LDOS)

T-Matrix

single rotationally invariant defect in a 2D free electron gas

Fourier series expansion with respect to the scattering angle

$$T(k', k, \cos\phi) = T_0(k', k) + 2\sum_{m=1}^{\infty} T_m(k', k)\, \cos m\phi$$

for an isotropic system leads to a set of decoupled 1D integral equations

$$T_m(k', k) = v_m(k', k) + \int_0^{\infty} \frac{dp\, p}{2\pi}\, v_m(k', p)\, G_k^0(p)\, T_m(p, k)\,.$$

T-Matrix

single rotationally invariant defect in a 2D free electron gas

Fourier series expansion with respect to the scattering angle

$$T(k', k, \cos\phi) = T_0(k', k) + 2\sum_{m=1}^{\infty} T_m(k', k)\, \cos m\phi$$

for an isotropic system leads to a set of decoupled 1D integral equations

$$T_m(k', k) = v_m(k', k) + \int_0^{\infty} \frac{dp\, p}{2\pi}\, v_m(k', p)\, G_k^0(p)\, T_m(p, k)\,.$$

$T_m(k' = k, k)$ **can be expressed in terms of a real scattering phase shifts:**

$$T_m(k, k) = \frac{2}{\mu}\, \frac{1}{\cot\delta_m + i}$$

T-Matrix

single rotationally invariant defect in a 2D free electron gas

Fourier series expansion with respect to the scattering angle

$$T(k', k, \cos\phi) = T_0(k', k) + 2\sum_{m=1}^{\infty} T_m(k', k)\, \cos m\phi$$

for an isotropic system leads to a set of decoupled 1D integral equations

$$T_m(k', k) = v_m(k', k) + \int_0^{\infty} \frac{dp\, p}{2\pi}\, v_m(k', p)\, G_k^0(p)\, T_m(p, k)\,.$$

$T_m(k' = k, k)$ **can be expressed in terms of a real scattering phase shifts:**

$$T_m(k, k) = \frac{2}{\mu}\, \frac{1}{\cot\delta_m + i}$$

This is an excellent check for numerical calculations!

T-Matrix

single rotationally invariant defect in a 2D free electron gas

Fourier series expansion with respect to the scattering angle

$$T(k', k, \cos\phi) = T_0(k', k) + 2\sum_{m=1}^{\infty} T_m(k', k)\, \cos m\phi$$

for an isotropic system leads to a set of decoupled 1D integral equations

$$T_m(k', k) = v_m(k', k) + \int_0^{\infty} \frac{dp\, p}{2\pi}\, v_m(k', p)\, G_k^0(p)\, T_m(p, k)\,.$$

$T_m(k' = k, k)$ **can be expressed in terms of a real scattering phase shifts:**

$$T_m(k, k) = \frac{2}{\mu}\, \frac{1}{\cot\delta_m + i}$$

This is an excellent check for numerical calculations!
These relations do not hold for the generalized T-matrix

Results: Scattering Phase Shifts

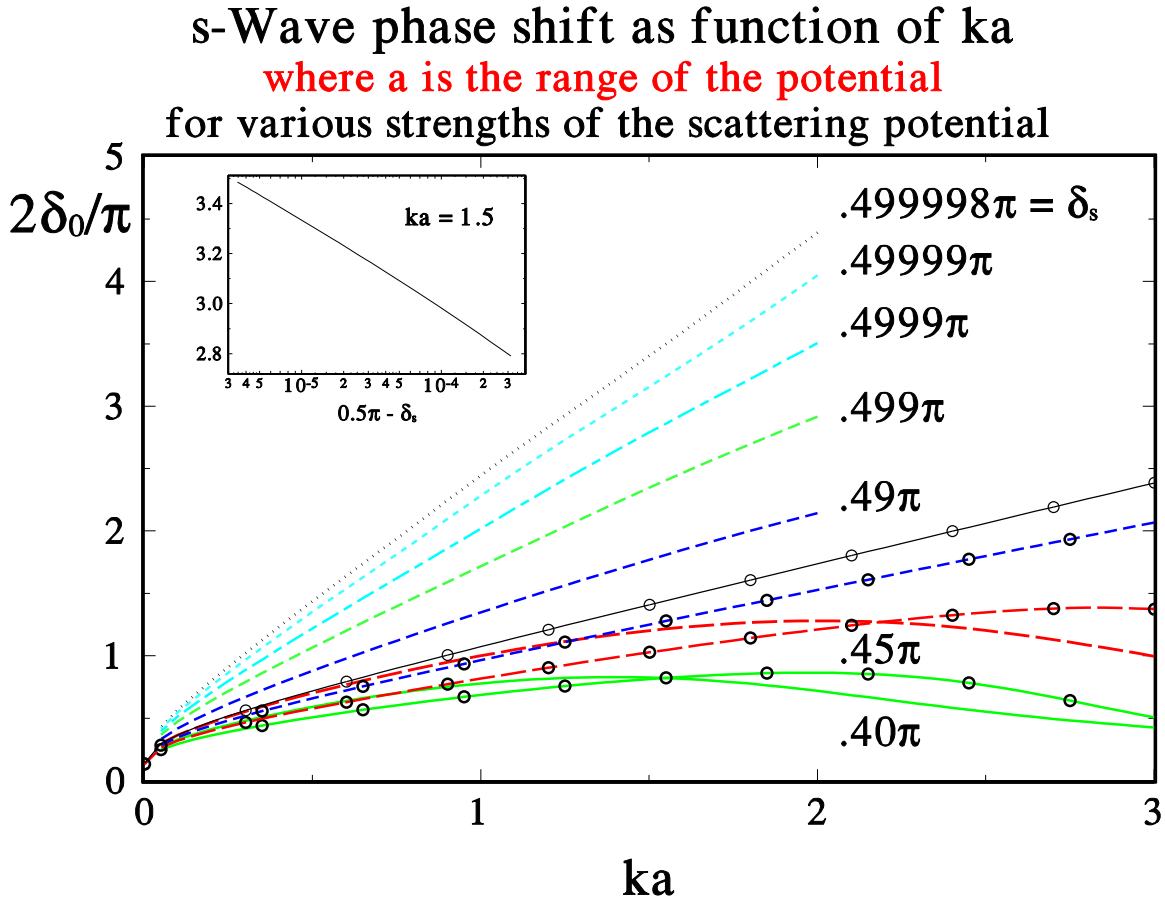

Curves marked with a circle are the results for a disk, the unmarked ones are for a Gaussian potential. The numbers are the phase shifts $\tan \delta_s = \pi \mathcal{N} \bar{v}$ characterizing the strength of the scattering potential.

Results: Scattering Phase Shifts

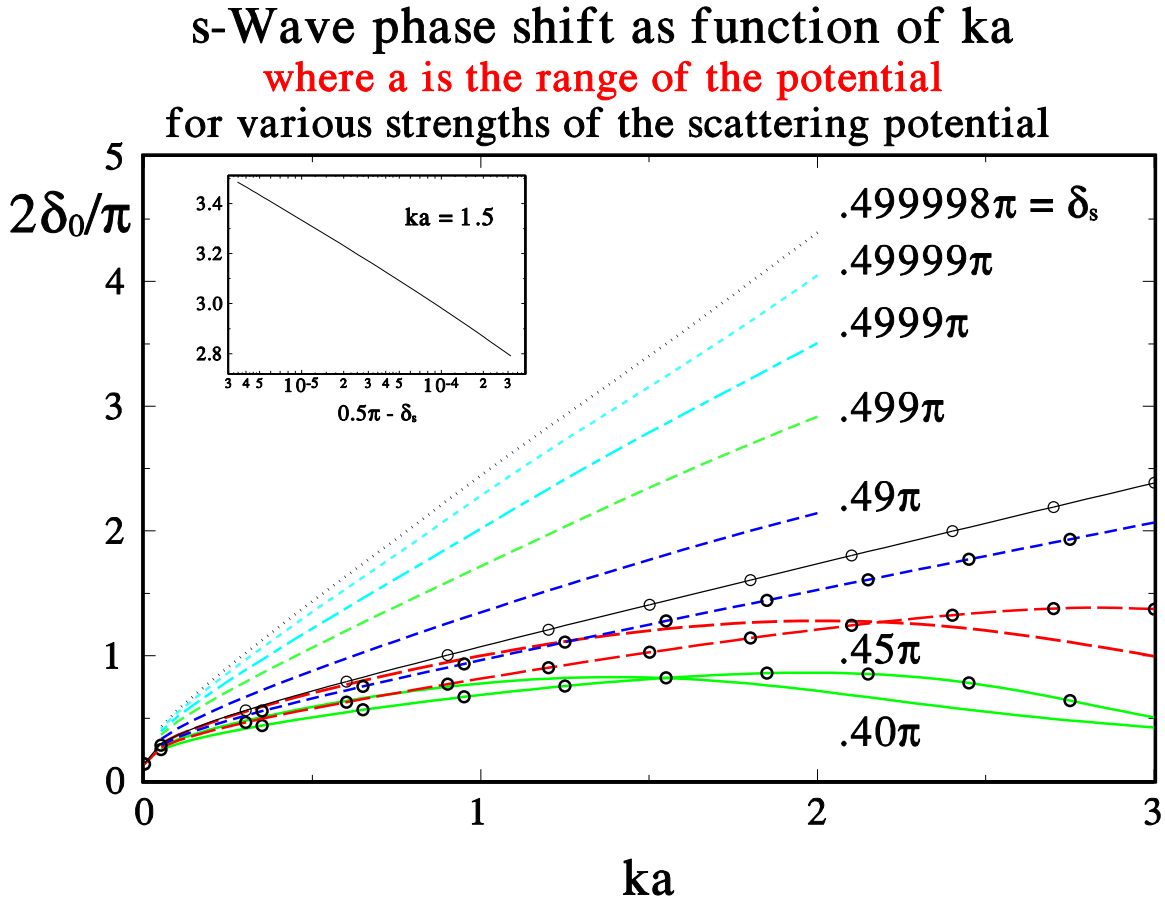

Curves marked with a circle are the results for a disk, the unmarked ones are for a Gaussian potential. The numbers are the phase shifts $\tan \delta_s = \pi \mathcal{N} \bar{v}$ characterizing the strength of the scattering potential.

For $a \longrightarrow 0$, the T-matrix vanishes logarithmically!

Local Density of States: Disk

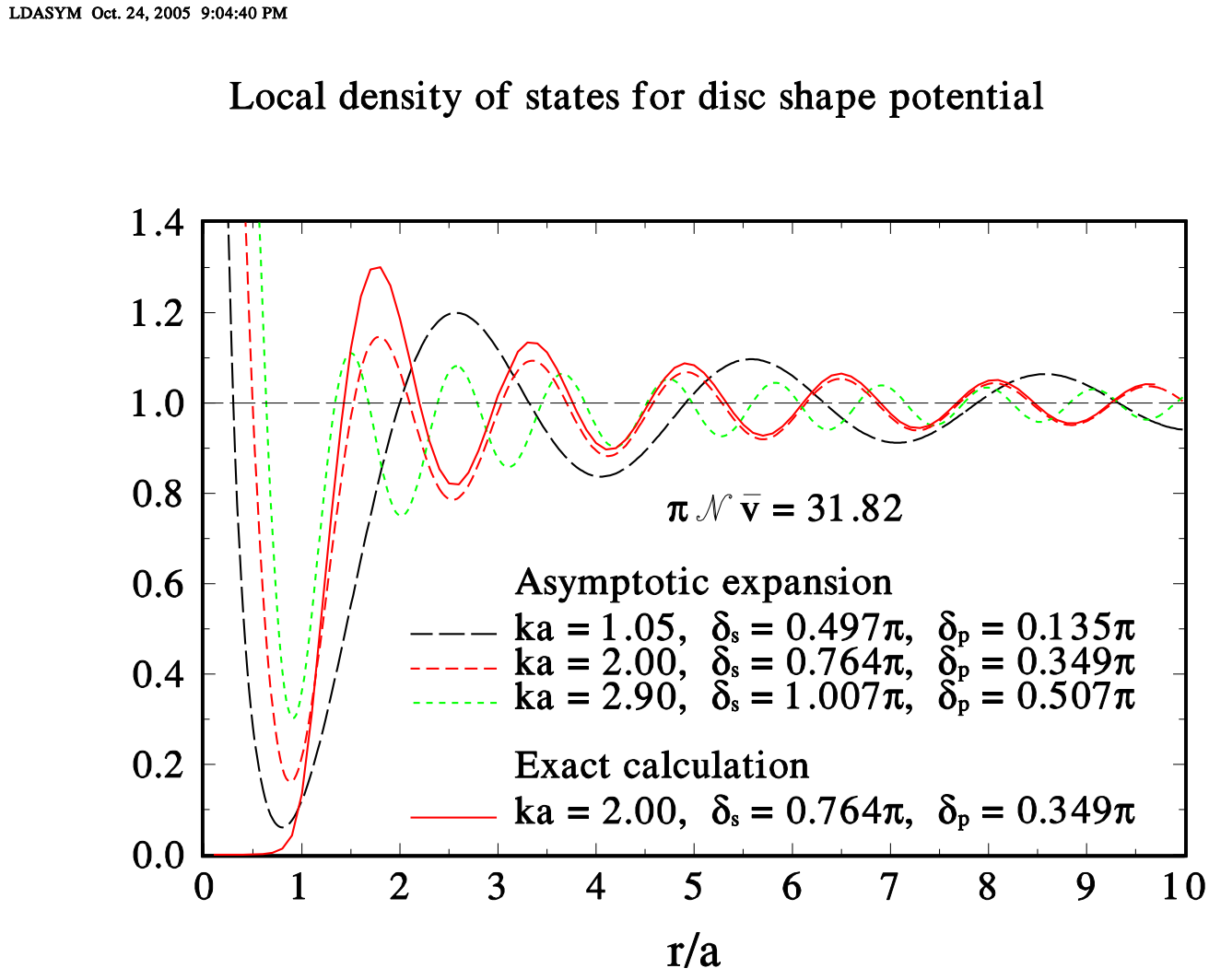

Note the difference between the exact and the asymptotic calculation for $r/a < 1$ and the large Friedel oscillations in 2D

Local Density of States: Gaussian

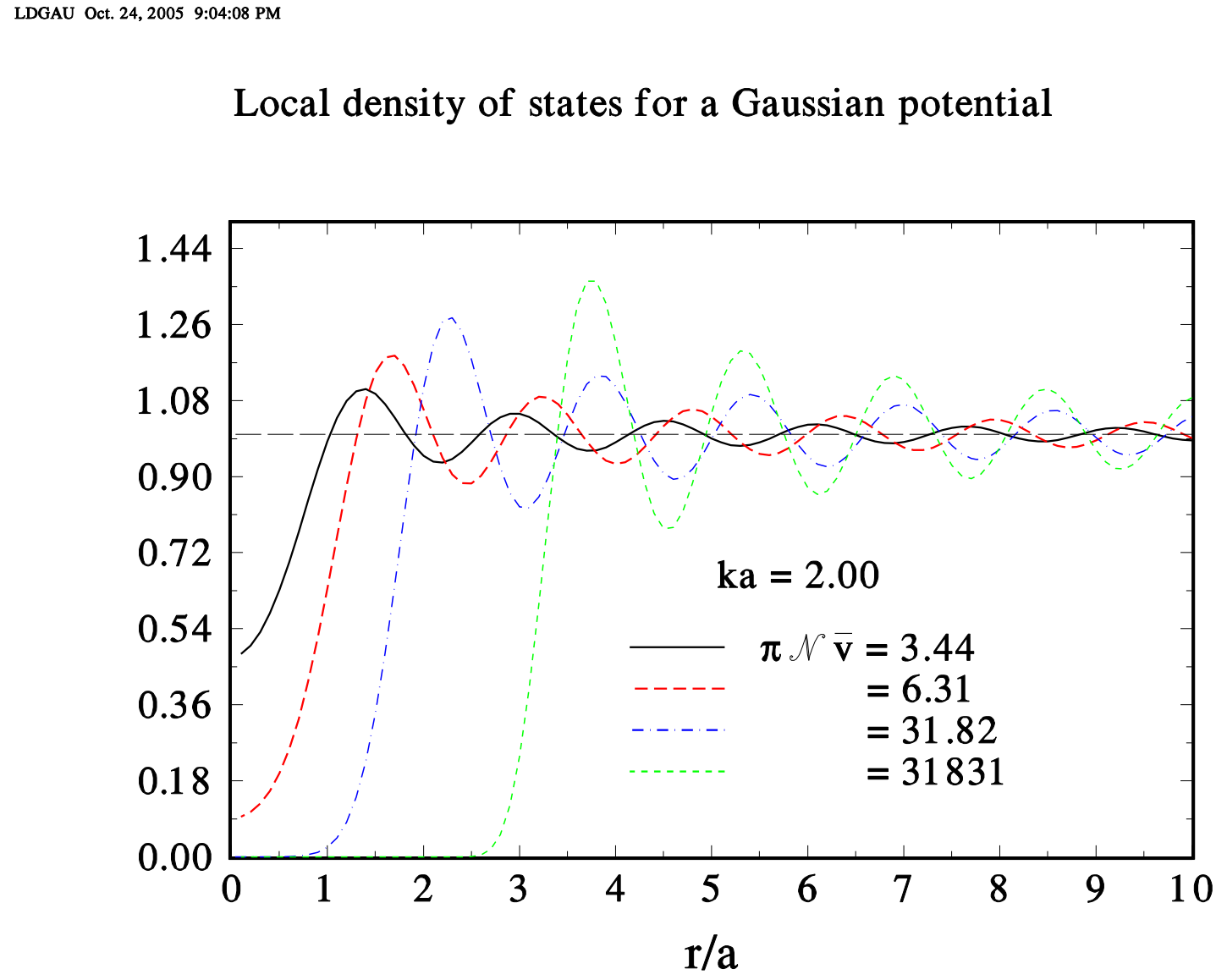

The LDOS for a fixed energy $ka = 2.00$ and different potential strength

GRAPHENE

Equation of motion for the Green functions in integral form revisited:

$$\hat{G}(\mathbf{r},\mathbf{r}';\omega) = \hat{G}^0(\boldsymbol{r}-\boldsymbol{r'};\omega) + \int d^2\rho\, \hat{G}^0(\boldsymbol{r}-\boldsymbol{\rho};\omega)\, \hat{V}(\boldsymbol{\rho})\, \hat{G}(\boldsymbol{\rho},\boldsymbol{r'};\omega)$$

Given $\hat{G}^0(\mathbf{r}-\mathbf{r}';\omega)$ and $\hat{V}(\boldsymbol{\rho})$, this could be solved directly.

For $\hat{V}(\boldsymbol{\rho}) = \hat{V}\,\delta(\boldsymbol{\rho})$, the solution is trivial:

$$\hat{G}(\boldsymbol{r},\boldsymbol{r'};\omega) = \hat{G}^0(\boldsymbol{r}-\boldsymbol{r'};\omega) + \hat{G}^0(\boldsymbol{r};\omega)\,\hat{V}\left(\hat{\sigma}_0 - \hat{G}^0(0;\omega)\,\hat{V}\right)^{-1}\hat{G}^0(-\mathbf{r}';\omega)$$

This equation was used to calculate the LDOS of graphene, invoking a finite band width. [a]

$\hat{G}^0$ and $\hat{V}$ are 2×2 matrices because Graphene has a lattice with a basis. The scattering potential is

$$\hat{V}_s = \begin{pmatrix} U_0 & 0 \\ 0 & 0 \end{pmatrix} \quad \textbf{and} \quad \hat{V}_d = \begin{pmatrix} U_0 & U_1 \\ U_1 & U_0 \end{pmatrix}$$

for a single impurity and for two identical impurities occupying neighbouring sites on the two sublattices, respectively. In the latter case, the hopping between these two lattice sites is likely to be modified, which is taken into account by the parameter U_1.

---

[a] T. O. Wehling et al., Phys. Rev. B75 (2007) 125425

Graphene - Crystal Structure

Honeycomb crystal structure of graphene. There are two atoms per primitive unit cell or, alternatively, two degenerate sublattices A and B.

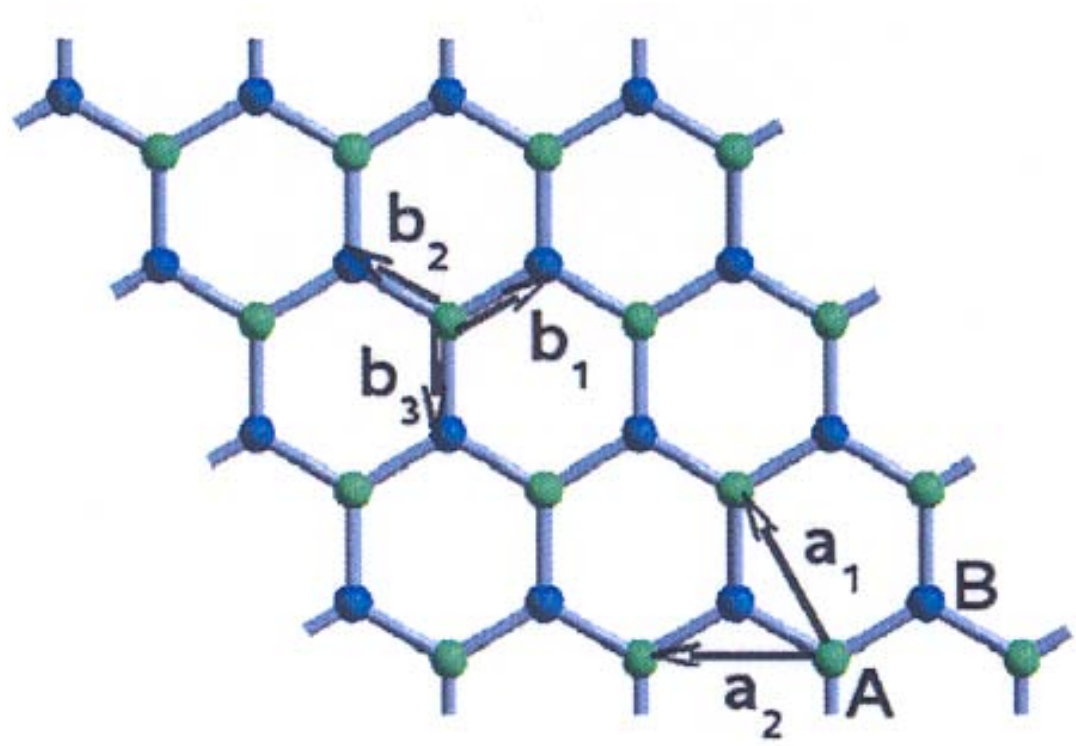

Graphene - Band Structure

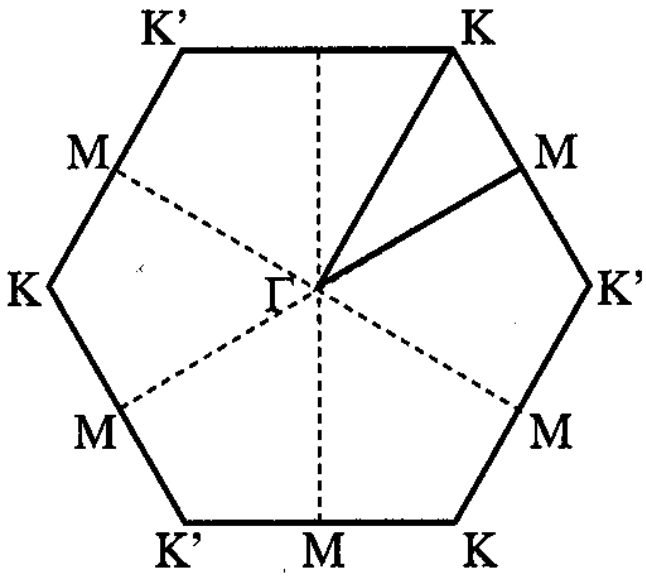

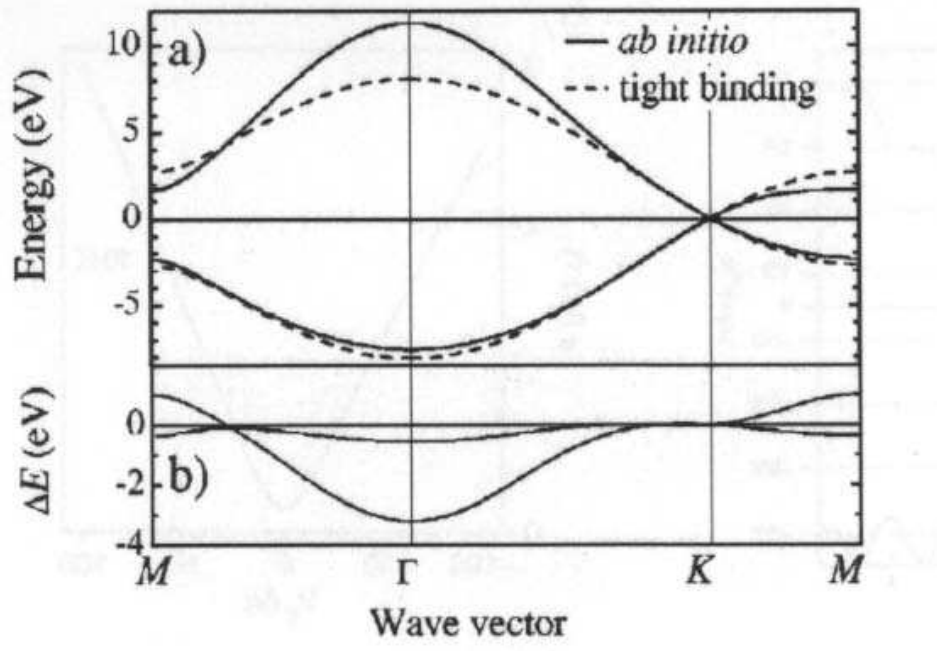

The band formed from p_z orbitals intersects the Fermi energy at the K-point. $\rightarrow$ The dispersion near K is linear! $\rightarrow$ massless fermions!

There is some similarity here with nodal quasiparticles in high-T_c superconductors.

Graphene - Green Function

$$\hat{G}^0(\mathbf{k},\omega) = \frac{1}{\omega_+^2 - |\xi(\mathbf{k})|^2} \begin{pmatrix} \omega & \xi(\mathbf{k}) \\ \xi^*(\mathbf{k}) & \omega \end{pmatrix}$$

$$\xi(\mathbf{k}) \approx t\left(1 + e^{i\mathbf{k}\cdot(\mathbf{b}_2-\mathbf{b}_1)} + e^{i\mathbf{k}\cdot(\mathbf{b}_3-\mathbf{b}_1)}\right)$$

within a tight binding approximation

A double integral over this singular integrand has to be performed to obtain the desired Green function $\hat{G}^0(\boldsymbol{r};\omega)$ in position space.

Results: Single Impurity

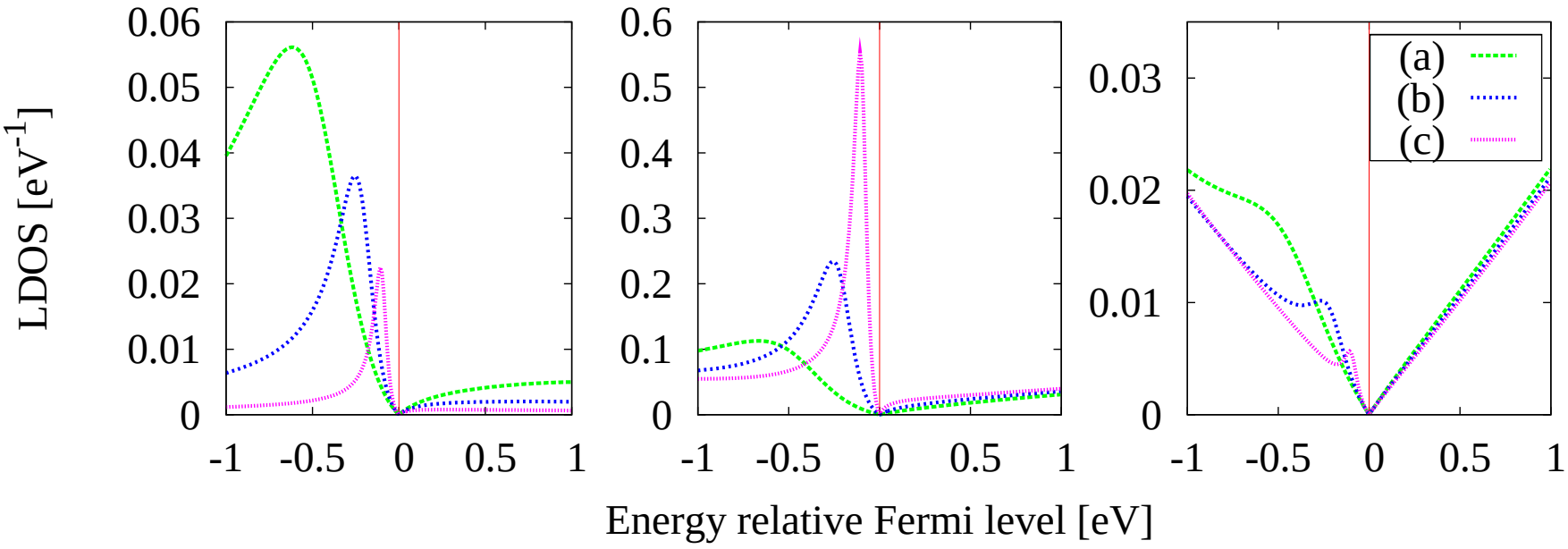

on-site

nearest neighbour

next nearest neighbour

(a) $V = 10$ eV,

(b) $V = 20$ eV,

(c) $V = 40$ eV,

Results: Double Impurity

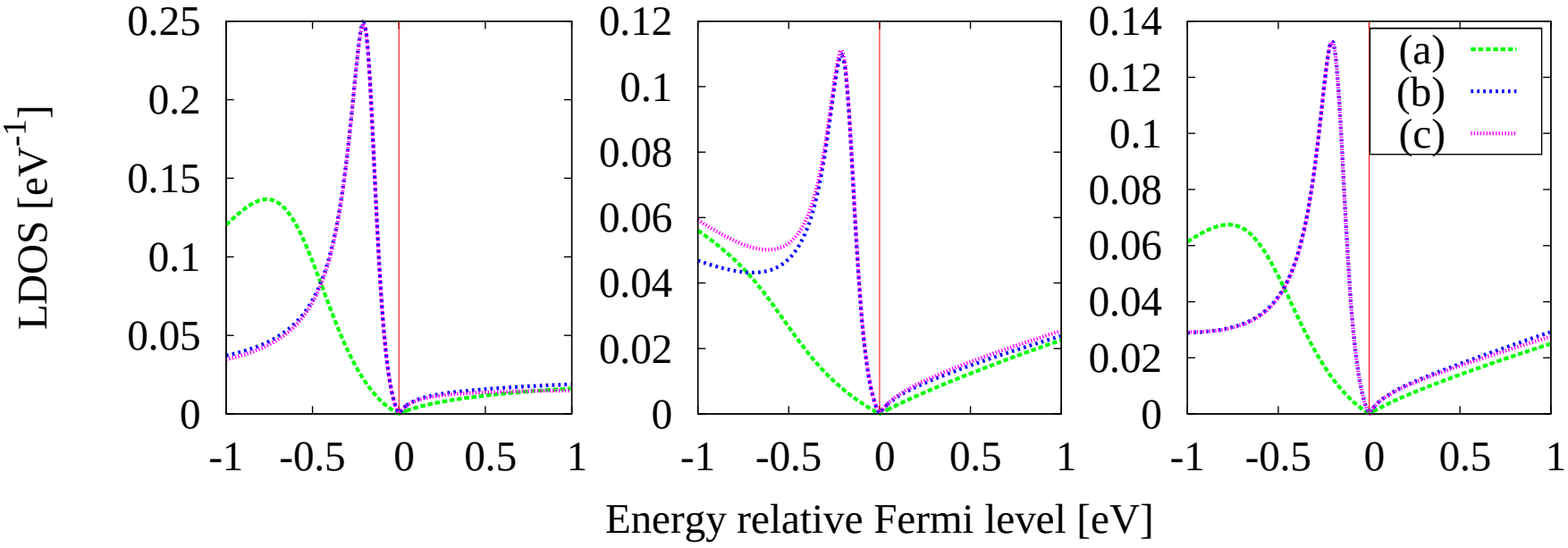

on-site | nearest neighbour | next nearest neighbour

(a) $V = 4$ eV, (b) $V = 4$ eV, $V_1 = -2$ eV (c) $V = 6$ eV,

V_1 is the change in the hopping matrix element, when two neighbouring sites are occupied by impurities.

When $V - V_1$ is kept constant, results are very similar! [(b) and (c)]

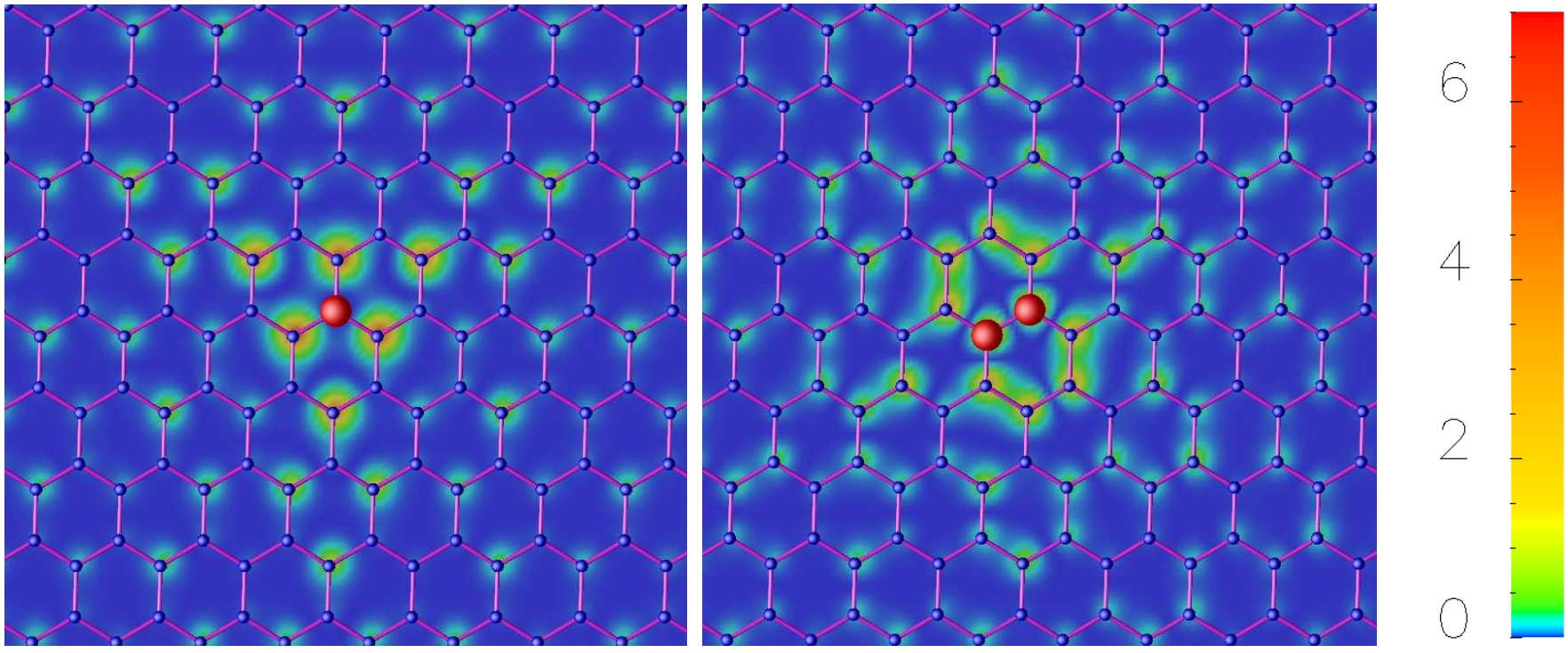
6
4
2
0

Comments on real space calculations on a lattice

Defect Hamiltonian in 2nd quantization for a single band:

$$H_D = \int d^D r\, \psi^+(\mathbf{r})\, \mathbf{V}(\mathbf{r})\, \psi(\mathbf{r})$$

Expand in terms of Bloch states : $H_D = \sum_{\mathbf{k},\mathbf{k}'} V(\mathbf{k},\mathbf{k}')\, c^+_{\mathbf{k}} c_{\mathbf{k}'}$

with $V(\mathbf{k},\mathbf{k}') = \int d^D r e^{-i(\mathbf{k}-\mathbf{k}')} u^*_{\mathbf{k}}(\mathbf{r})\, V(\mathbf{r}) u_{\mathbf{k}'(\mathbf{r})}$

Expand in terms of Wanier states: $H_D = \sum_{\ell,\ell'}\ V_{\ell,\ell'}\, c^+_{\ell} c_{\ell'}$

with $V_{\ell,\ell'} = \int d^D r\, w^*(\mathbf{r}-\mathbf{R}_\ell)\, V(\mathbf{r})\, w(\mathbf{r}-\mathbf{R}_{\ell'})$

This is a three-center integral!
Substantial simplification is achieved only if all but one-center intergrals can be neglected.
For this the potential has to be short ranged, but there is no advantage in assuming a δ-function. However, no matter how short-ranged the potential is, two- and three-center integrals have to be kept if the Wannier functions sufficiently overlap. Their overlap cannot be neglected because we are considering a metal.
There are two types of two-center integrals: In one of them $\mathbf{R}_\ell = \mathbf{R}'_\ell$ but different from the origin where the defect is located. So, on neighboring sites the on-site energy is changed which one would describe as the defect having a finite range. The second possibility is to have one Wannier function located on the defect site and the second one on some neighboring site. This corresponds to a modification of the hopping matrix elements betwen the defect site and neighboring sites. Three-center integrals describe changes in the hopping in the vicinity of the defect. Such changes in the hopping matrix elements could (and should) also be invoked on the grounds of the difference in size between host and defect atoms.
Considering all these ramifications, together with the possibility of having several Wannier states per site, would make these calculations exact but intractable. Our aim is to compare the tight-binding approximation with the NFE description to establish their relative merits for interpreting experimental results.